Observation of coherent phonons in strontium titanate: Structural phase transition and ultrafast dynamics of the soft modes

Kohmoto, Toshiro

Tada, K.

Moriyasu, T.

Fukuda, Yukio

(Citation)
Physical Review B,74(6):64303-64303

(Issue Date)
2006-08

(Resource Type)
journal article

(Version)
Version of Record

(URL)
https://hdl.handle.net/20.500.14094/90000235

Observation of coherent phonons in strontium titanate: Structural phase transition and ultrafast dynamics of the soft modes

T. Kohmoto,[1] K. Tada,[1] T. Moriyasu,[2] and Y. Fukuda[1]
[1]*Department of Physics, Faculty of Science, Kobe University, Kobe 657-8501, Japan*
[2]*Graduate School of Science and Technology, Kobe University, Kobe 657-8501, Japan*
(Received 20 March 2006; revised manuscript received 22 May 2006; published 10 August 2006)

Coherent phonons were observed in $SrTiO_3$ by using ultrafast polarization spectroscopy. The ultrafast dynamics and softening of phonon modes, which contribute to the structural phase transition at 105 K, are studied. The temperature dependences of the phonon frequency and the relaxation rate are obtained from the observed damped oscillation of coherent phonons. The observed phonon relaxation is explained well by a population decay due to anharmonic phonon-phonon coupling for the soft mode phonons.

DOI: 10.1103/PhysRevB.74.064303 PACS number(s): 77.84.Dy, 78.47.+p, 63.20.Kr

I. INTRODUCTION

Strontium titanate ($SrTiO_3$) is a well-known quantum paraelectric material. Its dielectric constant increases extraordinarily with decreasing temperature, while the paraelectric phase is stabilized by quantum fluctuations without a ferroelectric phase transition. The dielectric property and the lattice dynamics have been extensively studied. Recently, ferroelectricity induced by the isotopic substitution[1] of oxygen-18 for oxygen-16 and strong enhancement of the dielectric constant by uv-light irradiation[2,3] were discovered, and deeper interest has been taken in $SrTiO_3$ again.

$SrTiO_3$ is also known to undergo a structural phase transition at $T_c=105$ K.[4] The crystal has a cubic perovskite structure (O_h) above T_c, where all phonon modes are Raman forbidden. The crystal structure changes into tetragonal (D_{4h}) below T_c, where Raman-allowed modes of symmetries A_{1g} and E_g appear.[5] The phase transition is due to the collapse of the Γ_{25} mode at the R point of the high-temperature cubic Brillouin zone. Below T_c, the R point becomes the Γ point of the D_{4h} phase. The phase transition is characterized by the softening of phonons at the R point and concomitant doubling of the unit cell.

The distortion consists of an out-of-phase rotation of adjacent oxygen octahedra in the (100) planes.[4] The order parameter for the phase transition is inferred to be the angle of rotation of the oxygen octahedra. Only a small rotation of the oxygen octahedra is involved for the transition. The rotation angle for the oxygen octahedra varies from $\sim 2°$ of arc near 0 K down to zero at $T_c=105$ K; the transition is second order. At liquid nitrogen temperature, the rotation angle is about 1.4° and the linear displacement of the oxygen ions about their high-temperature equilibrium positions is less than 0.003 nm. This oxygen octahedron motion can be described as a rotation only as a first approximation; the oxygen ions actually remain on the faces of each cube and therefore increase in separation from the titanium. Because the (100) planes are equivalent in the cubic phase, the distortion produces domains below T_c in which the [100], [010], or [001] axis becomes the unique tetragonal c axis.

Optical information on the dielectric response is usually obtained from the Raman scattering or the infrared spectroscopy experiments. Observations of coherent phonons have also been demonstrated to be very useful for the investigation of low-frequency dielectric response. The time-resolved study of the dynamics of phonons[6] and phonon polaritons[7] turns out to be a very good probe for the properties of the low-frequency optical phonons. At low frequencies this technique is very sensitive and gives a superior signal-to-noise ratio compared to the conventional frequency-domain techniques, while at higher frequencies the conventional techniques will show a better performance. Hence the coherent phonon spectroscopy and the conventional frequency-domain techniques can be considered to be complementary methods for the investigation of the dielectric response.

The observed signal of the Raman scattering[8] in $SrTiO_3$ is very weak because the distortion from cubic structure in the low-temperature phase is very small. The intensity of the first-order Raman signal is of the same order of magnitude with many second-order Raman signals, and then a background-free signal of the first-order Raman scattering cannot be observed.

In the present work, ultrafast polarization spectroscopy is used to observe the coherent optical phonons in $SrTiO_3$, which are created by femtosecond optical pulses through the process of impulsive stimulated Raman scattering.[9,10] Time-dependent linear birefringence induced by the created coherent phonons is detected as a change of the polarization of probe pulses. High detection sensitivity of $\sim 10^{-5}$ in polarization change has been achieved in our detection system. We show that our approach in the time domain is very useful for the study of the soft phonon modes. Damped oscillations of coherent phonons were observed, and temperature dependences of the phonon frequency and the relaxation rate are measured. The mechanism of the phonon relaxation is discussed by using a population decay model, in which an optical phonon decays into two acoustic phonons due to anharmonic phonon-phonon coupling.

II. EXPERIMENT

Coherent phonons and their softening observed in the time domain are studied by ultrafast polarization spectroscopy with the pump-probe technique. The pump pulse is provided by a Ti:sapphire regenerative amplifier and the probe pulse by an optical parametric amplifier. The linearly polar-

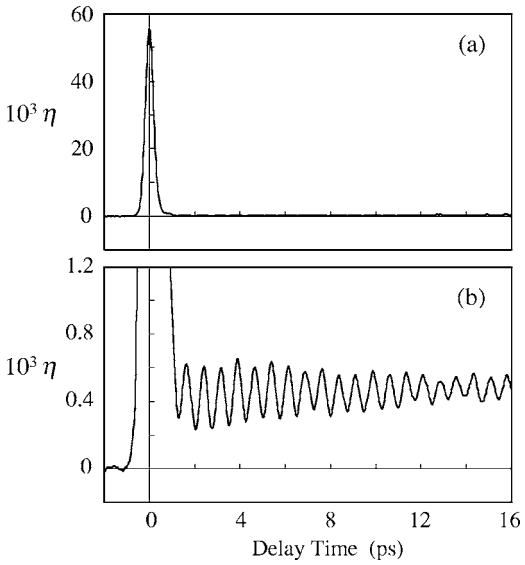

FIG. 1. Observed transient birefringence at 6 K for 0° pumping. The vertical axis is the ellipticity η in electric-field amplitude of the transmitted probe pulse. (a) A large signal due to the optical Kerr effect appears at zero delay. (b) Damped oscillation of coherent phonons follows after the Kerr signal. The vertical axis of (b) is enlarged by 50 from that of (a).

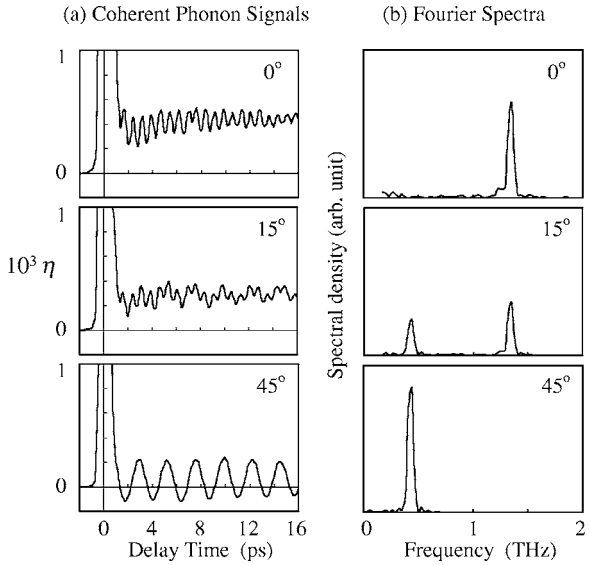

FIG. 2. (a) Coherent phonon signals at 6 K observed for 0°, 15°, and 45° pumping, where the angle between the [100] axis of the crystal and the polarization direction of the pump pulse is changed. (b) Fourier transform of the coherent phonon signals in (a).

ized pump and probe beams are nearly collinear and focused on the sample in a temperature-controlled refrigerator. The waist size of the beams at the sample is about 0.5 mm. The thickness of the sample is 1 mm, and the direction of the laser beams is perpendicular to the (001) surface. The wavelength, the pulse energy, and the pulse width at the sample are 790 nm, 2 μJ, and 0.2 ps for the pump pulse, and 690 nm, 0.1 μJ, and 0.2 ps for the probe pulse. The repetition rate of the pulses is 1 kHz.

Coherent phonons are created by the pump pulse through the process of impulsive stimulated Raman scattering, and induce time-dependent anisotropy of refractive index. The induced anisotropy of refractive index, linear birefringence, due to the created coherent phonons is detected by a polarimeter[11–13] with a quarter-wave plate as the change of the polarization of the probe pulse, whose plane of polarization is tilted by 45° from that of the pump pulse. The wavelengths of the pump and probe pulses can take any values in visible or near-infrared regions in the present experiment. We used two different wavelengths for the pump and probe pulses to eliminate the leak of the pump light from the input of the polarimeter by using interference filters.

The time evolution of the signal was observed by changing the optical delay between the pump and probe pulses. To improve the signal-to-noise ratio, the pump pulse was switched on and off shot by shot by using a photoelastic modulator with a quarter-wave plate and a polarizer, and the output signal from the polarimeter was lock-in detected.

III. RESULTS

Figure 1 shows the transient birefringence at 6 K observed for 0° pumping, where the polarization direction of the pump pulse is parallel to the [100] axis of the crystal. Vertical axis is the ellipticity η in electric-field amplitude of the transmitted probe pulse. At zero delay, a large signal due to the optical Kerr effect, whose width is determined by the pulse width, appears. After that, damped oscillation of coherent phonons is observed as shown in Fig. 1(b), where the vertical axis is enlarged by 50 from that of Fig. 1(a). The change of the polarization for the oscillation amplitude of the coherent phonon signal is 4×10^{-4} of the electric-field amplitude of the probe pulse, which corresponds to the change $\Delta n=7\times10^{-8}$ of the refractive index. In our detection system, polarization change of $\sim10^{-5}$ in the electric field amplitude can be detected.

Angular dependence of the coherent phonon signal at 6 K is shown in Fig. 2(a), where the angle between the [100] axis of the crystal and the polarization direction of the pump pulse is 0°, 15°, and 45°. The angle between the polarization directions of the pump and probe pulses is fixed to 45°. The 0.7 ps period signal for 0° pumping disappears for 45° pumping, where the 2.3 ps period signal appears. The Fourier transform of the coherent phonon signals in Fig. 2(a) is shown in Fig. 2(b). Oscillation frequency of the signal for the 0° pumping is 1.35 THz, and that for 45° pumping is 0.4 THz. For other pumping angles both frequency components coexist in the coherent phonon signal. From the oscillation frequencies the 1.35 THz component is considered to correspond to the A_{1g} mode, and the 0.4 THz component to the E_g mode.[5]

In addition to the oscillation signal there exists a dc component. The dc component has a maximum amplitude for 0° pumping and minimum amplitude for 45° pumping. However, the creation mechanism is not clear at present. In the following we pay attention to the oscillation component.

The temperature dependence of the coherent phonon signal for 0° pumping, which corresponds to the A_{1g} mode, is shown in Fig. 3. The oscillation period and the relaxation

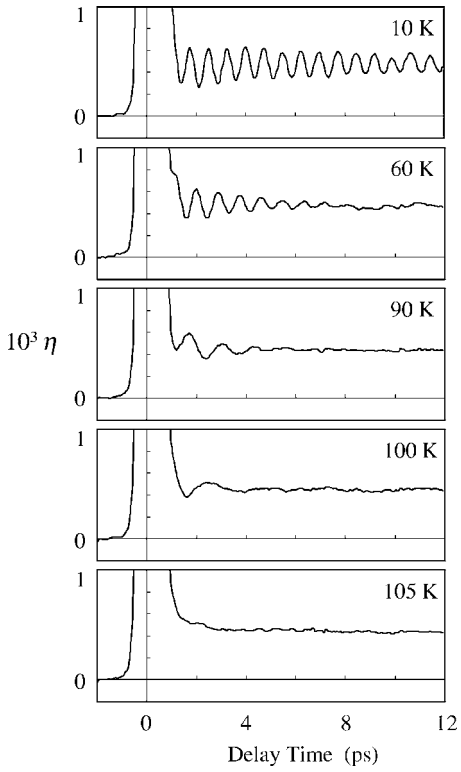

FIG. 3. Temperature dependence of the coherent phonon signal observed for 0° pumping, which corresponds to the A_{1g} mode.

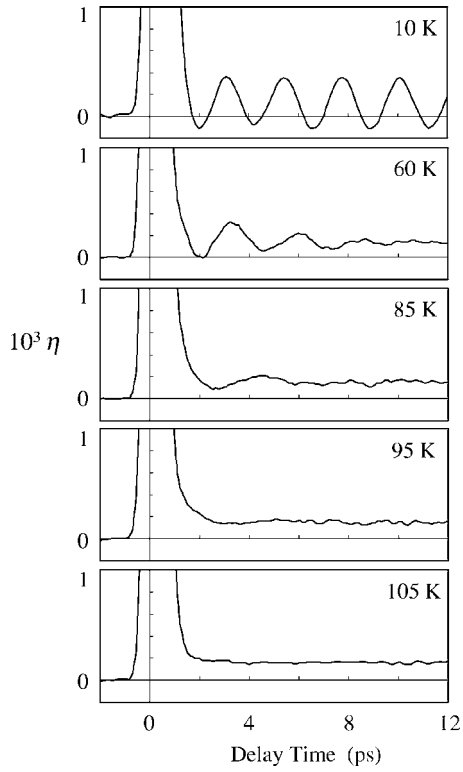

FIG. 4. Temperature dependence of the coherent phonon signal observed for 45° pumping, which corresponds to the E_g mode.

time of coherent phonons at 10 K are 0.7 and 12 ps. As the temperature is increased, the oscillation period becomes longer and the relaxation time becomes shorter. At $T_c = 105$ K, the phase transition point, the oscillation disappears. Above T_c no signal of coherent phonons is observed. The temperature dependence of the coherent phonon signal for 45° pumping, which corresponds to the E_g mode, is shown in Fig. 4. The oscillation period and the relaxation time of coherent phonons at 10 K are 2.3 and 45 ps. Similar behavior to that of the A_{1g} mode was observed as the temperature was increased.

IV. DISCUSSION

The observed coherent phonon signal $S(t)$ is expressed well by the damped oscillation

$$S(t) = Ae^{-\gamma t} \sin \omega t, \tag{1}$$

where ω is the oscillation frequency and γ is the relaxation rate. This sine-type function is expected for phonons induced by impulsive stimulated Raman scattering.[9,10] The temperature dependence of the oscillation frequency obtained from the observed coherent phonon signal below T_c is shown in Fig. 5. The solid circles are the oscillation frequency for the A_{1g} mode, and the solid squares are that for the E_g mode. As the temperature is increased from 6 K, the oscillation frequencies decrease and approach zero at the phase transition point T_c for both modes. This result is consistent with the temperature dependence of phonon frequency observed by Raman scattering.[5] The solid curves describe a temperature dependence of the form $\omega \propto (T_c - T)^n$. The experimental results for the temperature region between 50 K and T_c are explained well by $n = 0.4$ for both modes, while those below 40 K deviate from that form.

The intensity of the first-order Raman-scattering signal in $SrTiO_3$ is very weak and is of the same order of magnitude as many second-order Raman-scattering signals because the distortion from the cubic structure in the low-temperature

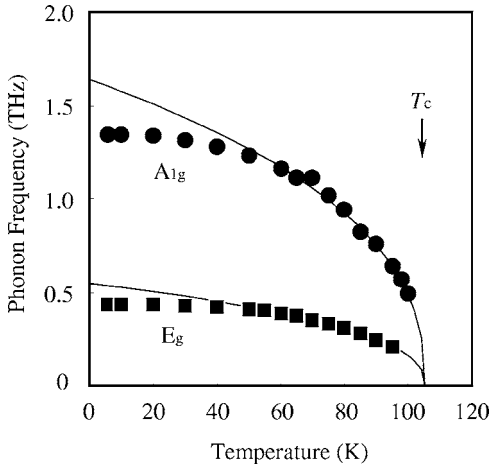

FIG. 5. Temperature dependence of the oscillation frequency obtained from the coherent phonon signal below T_c. The solid circles are the oscillation frequency for the A_{1g} mode, and the solid squares are that for the E_g mode. The solid curves describe a temperature dependence of the form $\omega \propto (T_c - T)^n$, where $T_c = 105$ K and $n = 0.4$ for both modes.

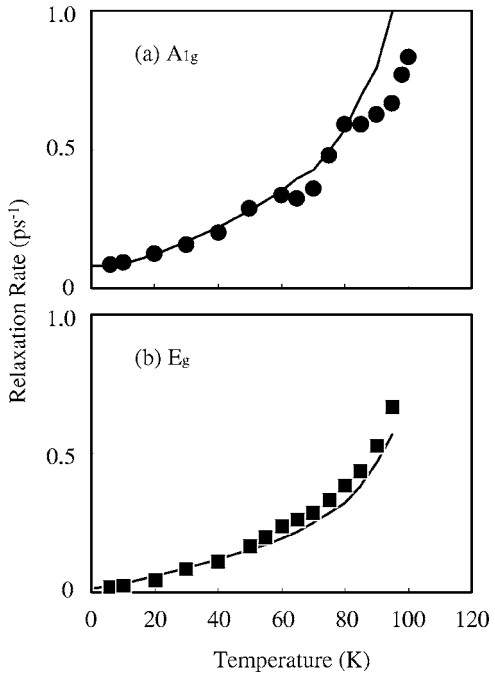

FIG. 6. Temperature dependence of the relaxation rate obtained from the coherent phonon signal below T_c. (a) The solid circles are the relaxation rate for the A_{1g} mode, and (b) the solid squares are that for the E_g mode. The solid curves show the theoretical curves including the frequency change obtained from Eq. (3), with γ_0 =(a) 8.0×10^{10} and (b) 1.5×10^{10} s^{-1}, where the observed phonon frequencies in Fig. 5 are used for each temperature.

phase is very small. Then observation of a background-free signal of first-order Raman scattering is not easy, and information on the relaxation, or the spectral width, is not given in a study of Raman scattering.[8] By the present method of coherent phonon spectroscopy in the time domain, on the other hand, background-free damped oscillations can be observed directly, and the oscillation frequency and the relaxation rate can be obtained accurately.

The temperature dependence of the relaxation rate obtained from the observed coherent phonon signal below T_c is shown in Fig. 6. The solid circles are the relaxation rate for the A_{1g} mode and the solid squares are that for the E_g mode. The relaxation rates increase as the temperature is increased.

In general, relaxation of coherent phonons is determined by population decay (inelastic scattering) and pure dephasing (elastic scattering). In metals, pure dephasing due to electron-phonon scattering, which depends on the hot electron density, contributes to the phonon relaxation.[14] In dielectric crystals, the relaxation process of the coherent phonon is considered to be dominated by the population decay due to the anharmonic phonon-phonon coupling,[15–17] rather than pure dephasing. According to the anharmonic decay model,[15] the relaxation of optical phonons in the center of the Brillouin zone is considered to occur through two types of decay process, the down-conversion and up-conversion processes. In a down-conversion process, the initial ω_0 phonon with wave vector $k\simeq0$ decays into two lower-energy phonons ω_i and ω_j, with opposite wave vectors k and $-k$, which belong to the i branch and the j branch of the phonon. Energy and wave-vector conservation is given by $\omega_0=\omega_{ik}+\omega_{j-k}$. In an up-conversion process, the initial excitation is scattered by a thermal phonon (ω_{ik}) into a phonon of higher energy (ω_{jk}), where $\omega_0+\omega_{ik}=\omega_{jk}$. The down-conversion process can be realized either for $i=j$ (overtone channel), or for $i\neq j$ (combination channel), depending on the phonon band structure of the material, while the up-conversion process contains only the combination channel and has no overtone channel. The combination channel is less likely, because three frequencies of phonons and three phonon branches have to be concerned and stringent limitations are imposed by the energy and wave-vector conservation. The overtone channel, on the other hand, is more likely because two (an optical and an acoustic) phonon branches are concerned, and the energy and wave-vector conservation are necessarily satisfied by two acoustic phonons with the same frequency and opposite wave vectors, if the frequency maximum of the acoustic branch is higher than half the frequency of the initial optical phonon.

Here we consider the down-conversion process in which an optical phonon decays into two acoustic phonons with half the frequency of the optical phonon and with opposite wave vectors. The temperature dependence of the relaxation rate γ of the coherent phonon is given by[15,16]

$$\gamma=\gamma_0\left(1+\frac{2}{\exp[(\hbar\omega_0/2)/k_BT]-1}\right), \tag{2}$$

where ω_0 is the frequency of the optical phonon, and k_B is the Boltzmann constant.

In ordinary materials the temperature dependence of the phonon frequency is small, and a theoretical curve with a fixed value of phonon frequency fits the experimental data well. In $SrTiO_3$, however, the phonon frequencies are changed greatly as the temperature is increased; thus a frequency change has to be considered. The solid curves in Fig. 6 show the theoretical curves including the frequency change obtained from Eq. (2) with $\gamma_0=8.0\times10^{10}$ s^{-1} for the A_{1g} mode and 1.5×10^{10} s^{-1} for the E_g mode, where the observed phonon frequencies in Fig. 5 are used for each temperature. As is seen in Fig. 6, the solid curves explain well the experimental data.

Deviation of the experimental data near T_c from the solid curve may be caused by the effect of the phase transition. However, the relaxation rate just around the phase transition point cannot be obtained in the present experiment, and the relation between the temperature-dependent relaxation rate and the structural phase transition is not clear.

V. SUMMARY

We have applied ultrafast polarization spectroscopy to observe coherent phonons in $SrTiO_3$, and showed that this approach in the time domain is very useful for the study of soft phonon modes. Coherent phonons are created by linearly polarized pump pulses. The time-dependent linear birefringence induced by the created coherent phonons is detected as a change of the polarization of the probe pulses. A high detection sensitivity of $\sim10^{-5}$ in polarization change, which

corresponds to the change $\Delta n = 2 \times 10^{-9}$ of the refractive index for a 1 mm sample, has been achieved in our detection system. Damped oscillations of coherent phonons for A_{1g} and E_g modes, which contribute to the structural phase transition at 105 K, were observed. The temperature dependences of the frequency and the relaxation rate of the observed coherent phonons were measured. Softening of the phonon frequencies was observed. The phonon relaxation is explained well by a decay model of a frequency-changing phonon, in which the optical phonon decays into two acoustic phonons due to the anharmonic phonon-phonon coupling.

ACKNOWLEDGMENTS

We would like to thank K. Tomizawa and H. Tanaka for experimental help in the earlier stage of the present experiment.

[1] M. Itoh, R. Wang, Y. Inaguma, T. Yamaguchi, Y-J. Shan, and T. Nakamura, Phys. Rev. Lett. **82**, 3540 (1999).
[2] M. Takesada, T. Yagi, M. Itoh, and S. Koshihara, J. Phys. Soc. Jpn. **72**, 37 (2003).
[3] T. Hasegawa, S. Mouri, Y. Yamada, and K. Tanaka, J. Phys. Soc. Jpn. **72**, 41 (2003).
[4] J. F. Scott, Rev. Mod. Phys. **46**, 83 (1974), and references therein.
[5] P. A. Fleury, J. F. Scott, and J. M. Worlock, Phys. Rev. Lett. **21**, 16 (1968).
[6] T. P. Dougherty, G. P. Wiederrecht, K. A. Nelson, M. H. Garrett, H. P. Jensen, and C. Warde, Science **258**, 770 (1992).
[7] H. J. Bakker, S. Hunsche, and H. Kurz, Rev. Mod. Phys. **70**, 523 (1998).
[8] W. G. Nilsen and J. G. Skinner, J. Chem. Phys. **48**, 2240 (1968).
[9] Y-X. Yan, E. B. Gamble, Jr., and K. A. Nelson, J. Chem. Phys. **83**, 5391 (1985).
[10] G. A. Garrett, T. F. Albrecht, J. F. Whitaker, and R. Merlin, Phys. Rev. Lett. **77**, 3661 (1996).
[11] T. Kohmoto, Y. Fukuda, M. Kunitomo, and K. Isoda, Phys. Rev. B **62**, 579 (2000).
[12] R. V. Jones, Proc. R. Soc. London, Ser. A **349**, 423 (1976).
[13] T. Kohmoto, Y. Fukuda, and T. Hashi, Phys. Rev. B **34**, 6085 (1986).
[14] K. Watanabe, N. Takagi, and Y. Matsumoto, Phys. Rev. Lett. **92**, 057401 (2004).
[15] F. Vallée, Phys. Rev. B **49**, 2460 (1994).
[16] M. Hase, K. Mizoguchi, H. Harima, S. I. Nakashima, and K. Sakai, Phys. Rev. B **58**, 5448 (1998).
[17] M. Hase, K. Ishioka, J. Demsar, K. Ushida, and M. Kitajima, Phys. Rev. B **71**, 184301 (2005).